Mechanism of the [RhF(PPh$_3$)$_3$] to *cis*-[RhPh(PPh$_3$)$_2$(PFPh$_2$)] Interconversion: P−C Activation and F/Ph Exchange via a Metallophosphorane Pathway

Stuart A. Macgregor* and Tebikie Wondimagegn

School of Engineering and Physical Sciences, William Perkin Building, Heriot-Watt University, Edinburgh EH14 4AS, U.K.

Received November 22, 2006

Density functional calculations have been carried out to model various pathways for F/Ph exchange in [RhF(PPh$_3$)$_3$]. Calculations on the full experimental system showed this process to occur via a novel pathway involving initial attack of fluoride on phosphine. This results in the formation of a metallophosphorane intermediate featuring a 5-coordinate phosphorus center. From this species P−Ph activation is very facile and leads to the F/Ph-exchanged product, *cis*-[RhPh(PPh$_3$)$_2$(PFPh$_2$)]. The computed activation energy of 22.3 kcal/mol is in excellent agreement with the experimental value. Alternative pathways based on initial Ph group transfer are significantly higher in energy. A key factor favoring the metallophosphorane route is the reduction in coordination number at the metal center that occurs in the initial fluoride transfer step; in contrast Ph group transfer creates a more sterically encumbered metal center. The metallophosphorane pathway indicates that "hard" donor species such as fluoride can induce facile P−C bond activation. This novel mechanism of phosphine ligand disruption may have general significance for the stability of transition metal−phosphine complexes in the presence of such species.

The use of phosphines in transition metal catalysis is usually founded on their acting as essentially innocent "spectators" while at the same time conferring a specific electronic, steric, or chiral environment on the metal center. Any process that compromises phosphine ligand structure is therefore usually highly undesirable. Such processes include the well-known orthometalation[1] and P−C bond cleavage reactions.[2] While orthometalation is often a reversible process and so may have a limited effect on catalysis, P−C bond cleavage, in contrast, can be highly damaging as it often leads to the formation of phosphido-bridged higher nuclearity species which exhibit reduced catalytic activity. Closely related to P−C bond cleavage are P−R/X exchange reactions.[3] In this case a phosphine substituent (R = aryl, alkyl) is replaced by another group, X (X = aryl,[4] alkyl,[5] NR$_2$,[6] OR,[7−9] F[10]). A phosphine ligand is therefore retained but now in a modified form as PR$_2$X. Such processes have been exploited in synthesis, most notably those involving aryl/aryl exchange.[4a,c,d,f] More generally, however, the alteration in the bonding character of the phosphine can have a detrimental effect on catalyst activity. Moreover, there are many examples in metal-mediated coupling reactions where P−Ph/X exchange leads to the

* To whom correspondence should be addressed. E-mail: s.a.macgregor@hw.ac.uk.

(1) (a) Cotton, F. A.; Wilkinson, G.; Murillo, C. A.; Bochmann, M. In *Advanced Inorganic Chemistry*; Wiley-Interscience: New York, 1999; p 1198. (b) Bruce, M. I. *Angew. Chem., Int. Ed Engl.* **1977**, *16*, 73.

(2) (a) Garrou, P. E. *Chem. Rev.* **1985**, *85*, 171. (b) Parkins, A. W. *Coord. Chem. Rev.* **2006**, *250*, 449.

(3) (a) Macgregor, S. A. *Chem. Soc. Rev.* **2006**, DOI:10.1039/B516248N.

(4) (a) de la Torre, G.; Gouloumis, A.; Vázquez, P.; Torres, T. *Angew. Chem., Int. Ed.* **2001**, *40*, 2895. (b) Grushin, V. V. *Organometallics* **2000**, *19*, 1888. (c) Kwong, F. Y.; Chan, K. S. *Organometallics* **2000**, *19*, 2058. (d) Kwong, F. Y.; Chan, K. S. *Chem. Commun*. **2000**, 1069. (e) Goodson, F. E.; Wallow, T. I.; Novak, B. M. *J. Am. Chem. Soc.* **1997**, *119*, 12441. (f) Sakamoto, M.; Shimizu, I.; Yamamoto, A. *Chem. Lett*. **1995**, 1011. (g) Segelstein, B. E.; Butler, T. W.; Chenard, B. L. *J. Org. Chem.* **1995**, *60*, 12. (h) Kong, K.-C.; Cheng, C.-H. *J. Am. Chem. Soc.* **1991**, *113*, 6313. (i) Dubois, R. A.; Garrou, P. E. *Organometallics* **1986**, *5*, 466. (j) Abatjoglou, A. G.; Bryant, D. R. *Organometallics* **1984**, *3*, 932. (k) Goel, A. B. *Inorg. Chim. Acta* **1984**, *86*, L77.

(5) (a) Morita, D. K.; Stille, J. K.; Norton, J. R. *J. Am. Chem. Soc.* **1995**, *117*, 8576. (b) Mohtachemi, R.; Kannert, G.; Schumann, H.; Chocron, S.; Michman, M. *J. Organomet. Chem.* **1986**, *310*, 107. (c) Abatjoglou, A. G.; Billig, E.; Bryant, D. R. *Organometallics* **1984**, *3*, 923. (d) Reference 4i. (e) Green, M. L. H.; Smith, M. J.; Felkin, H.; Swierczewski, G. *J. Chem. Soc., Chem. Commun*. **1971**, 158.

(6) (a) Vierling, P.; Riess, J. G.; Grand, A. *Inorg. Chem.* **1986**, *25*, 4144. (b) Al-Jibori, S.; MacDonald, W. S.; Shaw, B. L. *J. Chem. Soc., Chem. Commun*. **1982**, 287.

(7) P-C(sp^3)/OR exchange: (a) Cadierno, V.; Díez, J.; Garcia-Álvarez, J.; Gimeno, J. *Organometallics* **2004**, *23*, 3425. (b) Hartwig, J. F.; Bergman, R. G.; Andersen, R. A. *J. Organomet. Chem*. **1990**, *394*, 417. (c) Lin, I. J. B.; Lai, J. S.; Liu, C. W. *Organometallics* **1990**, *9*, 530. (d) Alcock, N. W.; Bergamini, P.; Kemp, T. J.; Pringle, P. G. *J. Chem. Soc., Chem. Commun*. **1987**, 235. (e) Bouaoud, S.-E.; Braunstein, P.; Grandjean, D.; Matt, D.; Nobel, D. *Inorg. Chem.* **1986**, *25*, 3765. (f) Al-Jibori, S.; Hall, M.; Hutton, A. T.; Shaw, B. L. *J. Chem. Soc., Chem. Commun*. **1982**, 1069.

(8) P-C(sp^2)/OR exchange: (a)Yasuda, H.; Maki, N.; Choi, J.-C.; Abla, M.; Sakakura, T. *J. Organomet. Chem.* **2005**, *691*, 1307. (b) Caballero, A.; Jalón, F. A.; Manzano, B. R.; Espine, G.; Pérez-Manrique, M.; Pobrete, F. J.; Maestro, M. *Organometallics* **2004**, *23*, 5694. (c) Setlef, D.; Baumann, W.; Kempe, R.; Spannenberg, A.; Röttger, D.; Wiese, K.-D.; Börner, A. *Organometallics* **2003**, *22*, 4265. (d) Geldbach, T. J.; Pregosin, P. S. *Eur. J. Inorg. Chem.* **2002**, *31*, 1907. (e) Crochet, P.; Demeuseman, B.; Rocaboy, C.; Schleyer, D. *Organometallics* **1996**, *15*, 3048. (f) van Leeuwen, P. W. N. M.; Roobeek, C. F.; Orpen, A. G. *Organometallics* **1990**, *9*, 2179. (g) Morris, R. H.; Sawyer, J. F.; Schweitzer, C. T.; Sella, A. *Organometallics* **1989**, *8*, 2099. (h) Cowie, M.; McKeer, I. R.; Loeb, S. J.; Gauthier, M. D. *Organometallics* **1986**, *5*, 860. (i) Chakravarty, A. K.; Cotton, F. A.; Tocher, D. A. *Inorg. Chem.* 1985, **24**, 3584. (j) Beck, W.; Keubler, M.; Leidl, E.; Nadel, U.; Schaal, M.; Cenini, S.; Del Buttero, P.; Licandro, E.; Mairana, S.; Vila, A. C. *J. Chem. Soc., Chem. Commun*. **1981**, 446. (k) Kikukawa, K.; Matsuda, T. *J. Organomet. Chem.* **1980**, *235*, 243.

(9) P−C(sp)/OR exchange: Naik, D. V.; Palenik, G. J.; Jacobson, S.; Carty, A. J. *J. Am. Chem. Soc.* **1974**, *96*, 2286.

(10) (a) Jasim, N. A.; Perutz, R. N.; Whitwood, A. C.; Braun, T.; Izundu, J.; Neumann, B.; Rothfeld, S.; Stammler, H.-G. *Organometallics* **2004**, *23*, 6140. (b) Reference 8d. (c) den Reijer, C. J.; Dotta, P.; Pregosin, P. S.; Albinati, A. *Can. J. Chem.* **2001**, *79*, 693. Blum, O.; Frolow, F.; Milstein, D. *J. Chem. Soc., Chem. Commun.* **1991**, 258. (d) Reference 8g.

10.1021/om0610703 CCC: $37.00
Publication on Web 01/24/2007

Scheme 1

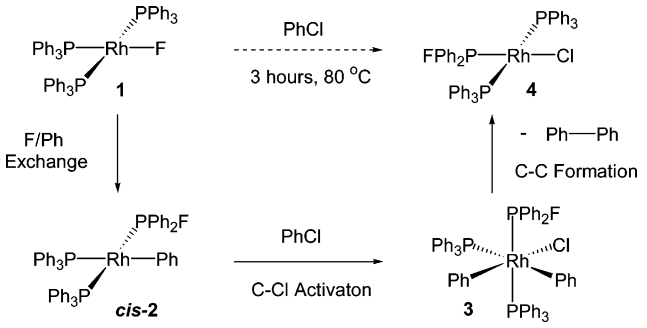

formation of undesirable side products, especially when X is another aryl group.[4g,11]

One particularly clear example of P−Ph/F exchange has been observed in [RhF(PPh_3)$_3$], **1**, the characterization of which was recently reported by Grushin and Marshall.[12] Upon heating of **1** in chlorobenzene a remarkable process involving Rh−F, P−C, and C−Cl bond cleavage and P−F, P−C, and C−C bond formation occurs to give *trans*-[RhCl(PPh_3)$_2$($PFPh_2$)], **4**, and biphenyl (Scheme 1). Subsequent mechanistic studies demonstrated that the novel reactivity of [RhF(PPh_3)$_3$] is initiated by an F/Ph exchange process to give *cis*-[RhPh(PPh_3)$_2$(PPh_2F)], *cis*-**2**.[13] *cis*-**2** is sufficiently electron-rich to activate chlorobenzene to give *cis*,*cis*-[RhCl(Ph)$_2$(PPh_3)$_2$(PPh_2F)], **3**, from which reductive elimination releases biphenyl and **4**. Kinetic studies revealed that the **1** to *cis*-**2** interconversion is a reversible intramolecular process, independent of PPh_3 concentration, with $\Delta H^{\ddagger} = 22.0 \pm 1.2$ kcal/mol and $\Delta S^{\ddagger} = -10.0 \pm 3.7$ eu. All this behavior is in sharp contrast to that exhibited under similar conditions by the chloro analogue, [RhCl(PPh_3)$_3$] (Wilkinson's catalyst), where precipitation of the chloro-bridged dimer [Rh$_2$(μ-Cl)$_2$(PPh_3)$_4$] formed via PPh_3 dissociation is observed.[14]

A range of mechanisms has been put forward for P−R/X exchanges of the type exemplified by the **1** to *cis*-**2** interconversion. These differ most fundamentally in the order of the transfer events (see Scheme 2). In pathway 1 exchange is initiated by attack of X at P (either intramolecularly, as shown, or externally). This is followed by R group transfer to M. The P−R/X exchange process may in principle be concerted (**A**), involve a metallophosphorane intermediate,[15] (**B**) or may involve the formation of a phosphonium salt (**C**). Experimental precedent is available for both intermediates **B** and **C**: Riess has characterized a metallophosphorane intermediate in a P−Ph/NR_2 exchange process on Fe,[6a] while phosphonium salts are implicated in P−aryl/aryl exchange processes on Pd.[4b−g] In pathway 2 exchange is initiated by P−C bond activation with R group transfer to M. This formal oxidative addition results in phosphido species (**D**) from which P−X bond-forming reductive elimination completes the P−R/X exchange.

In our previous study of [RhF(PPh_3)$_3$], we employed density functional (DF) calculations on a small model system,

Scheme 2

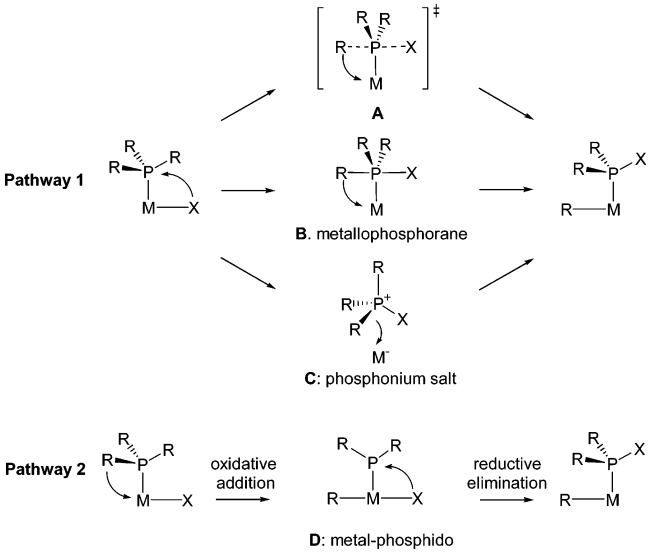

[RhF(PH_3)$_2$(PH_2Ph)], **1′**, to assess possible mechanisms for the F/Ph exchange reaction.[13] These were based on the two general processes outlined in Scheme 2, and within each pathway two variations were seen (see Scheme 3). Along pathway 1, the formation of a metallophosphorane species via initial F transfer to phosphine was found. This process could occur either with (pathway 1a) or without (pathway 1b) the concomitant movement of a second phosphine ligand, such that the [$PFPh_3$]$^-$ phosphoranide ligand formed is either trans or cis to the vacant site respectively. Along pathway 2, Rh−phosphido species were located via initial Ph to Rh transfer, a process that could occur either from a cis (pathway 2a) or trans (pathway 2b) phosphine. Formal P−F reductive elimination then completed F/Ph exchange, with both pathways 2a and 2b leading directly to *cis*-**2**. These calculations on the small [RhF(PH_3)$_2$(PH_2Ph)] model system showed three of the four possible mechanisms had very similar computed activation energies of around 31 kcal/mol with only pathway 1b, with an activation energy of 37 kcal/mol, lying to significantly higher energy. Thus, these calculations were inconclusive in terms of defining which of pathway 1 or 2 was the more likely mechanism for P−Ph/F exchange in **1**. In addition, the computed activation energies were all significantly higher than the experimental activation enthalpy of 22.0 ± 1.2 kcal/mol.

In this paper we have extended our computational studies to the full [RhF(PPh_3)$_3$] complex to discriminate between the various mechanistic possibilities presented by pathways 1 and 2. We show that the introduction of the PPh_3 ligands produces a clear preference for F/Ph exchange via the metallophosphorane structure of pathway 1a. In addition, the comparison of pathways 1 and 2 provides the opportunity for a reassessment of the P−Ph bond cleavage reaction. To our knowledge this fundamental process has been the subject of only one previous computational study. In this study, Hoffmann and co-workers employed extended Hückel calculations on model species of the type [Pd(H)$_3$(PH_2R)]$^-$ (R = Me, Ph)[16] to assess the ease of R group transfer from P to Pd. This process was shown to be more facile for R = Ph compared to Me, but while the comparison of relative barriers for this process is reasonable, it is likely that

(11) Further examples: (a) Herrmann, W. A.; Brossmer, C.; Öfele, K.; Beller, M.; Fischer, H. *J. Mol. Catal., A* **1995**, *103*, 133. (b) Barañano, D.; Hartwig, J. F. *J. Am. Chem. Soc*. **1995**, *117*, 2937. (c) Buszek, K. R.; Jeong, Y.-M. *Tetrahedron Lett.* **1995**, *36*, 5677. (d) O'Keefe, D. F.; Dannock, M. C.; Marcuccio, S. M. *Tetrahedron Lett.* **1992**, *33*, 6679.

(12) Grushin, V. V.; Marshall, W. J. *J. Am. Chem. Soc.* **2004**, *126*, 3026.

(13) Macgregor, S. A.; Roe, D. C.; Marshall, W. J.; Bloh, K. M.; Bakhmutov, V. I.; Grushin, V. V. *J. Am. Chem. Soc*. **2005**, *127*, 15304.

(14) Jardine, F. H. *Prog. Inorg. Chem.* **1981**, *28*, 63.

(15) For reviews on metallophosphorane chemistry, see: (a) Nakazawa, H.; Kubo, K.; Miyoshi, K. *Bull. Chem. Soc. Jpn.* **2001**, *74*, 2255. (b) Dillon, K. B. *Chem. Rev.* **1994**, *94*, 1441.

(16) Ortiz, J. V.; Havlas, Z.; Hoffmann, R. *Helv. Chim. Acta* **1984**, *67*, 1.

Scheme 3

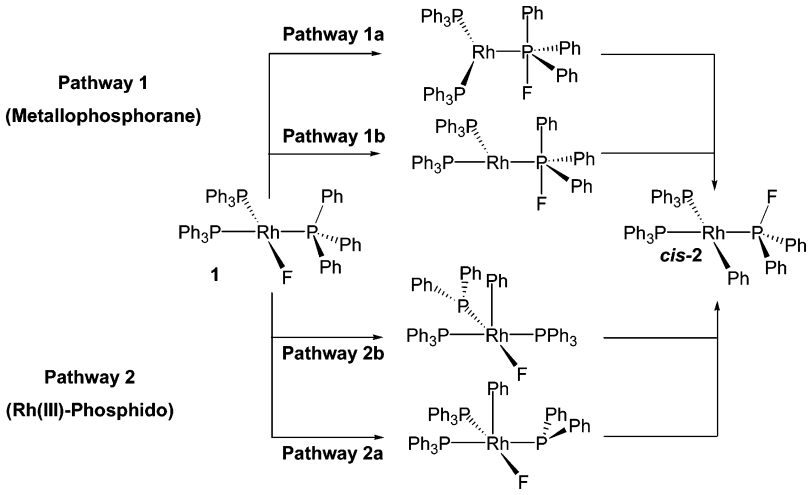

the absolute computed barriers are unreliable.[17] The present work therefore provides a high-level study of the fundamental P−Ph bond cleavage step and establishes that for **1** P−Ph activation via Ph group transfer from P to Rh is disfavored over a more accessible pathway involving a metallophosphorane intermediate. Our study suggests that the presence of "hard" donor species such as fluoride in **1** may induce P−C bond activation by attack at phosphorus. It also adds to the growing list of examples where metallophosphoranes play an important role as intermediates in transition metal chemistry.[6a,15,18]

Computational Details

To study the large [RhF(PPh$_3$)$_3$] system we have employed a combination of hybrid DF/Hartree−Fock and full DF calculations, and all geometries were optimized and characterized at the former level using the ONIOM scheme within Gaussian 03.[19] In this approach the full [RhF(PPh$_3$)$_3$] molecule is effectively divided into layers that are described at different levels of theory. In the present case a reactive [RhF(PH$_3$)$_2$(PH$_2$Ph)] core was defined and computed with the BP86 functional. For this layer Rh and P were described using the Stuttgart RECPs and the associated basis sets[20] with d-orbital polarization added for P (ζ = 0.387).[21] 6-31G** basis sets were used for C, F, and H atoms.[22] Within the ONIOM approach lower level Hartree−Fock calculations are required for both the full [RhF(PPh$_3$)$_3$] model and the [RhF(PH$_3$)$_2$(PH$_2$Ph)] small core model, and these used the LANL2DZ pseudopotentials[23] and basis sets for Rh and P (retaining the same d-orbital polarization on P as above), while C, F, and H atoms were described with the 6-31G basis set. All stationary points were fully characterized at the BP86/HF level via analytical frequency calculations as either minima (all positive eigenvalues) or transition states (one imaginary eigenvalue). Calculations were based on the published molecular structures of **1**[12] and *cis*-**2**,[13] although for all other stationary points the existence of alternative conformations was checked through the "scan" facility in the TINKER molecular mechanics program.[24] As IRC calculations are not available in Gaussian 03 for hybrid calculations, transition states were further characterized by displacing the geometry in such a way to mimic the unique imaginary frequency and then allowing these structures to relax to the adjacent local minima. The inclusion of zero-point energies and temperature effects was found to have only a minor effect on the key activation barriers, reducing all of these by between 1 and 1.5 kcal/mol at the BP86/HF level. Likewise entropic effects (298.15 K) were minimal with the exception of steps in pathways 2a and 2b involving phosphine dissociation (see text). The energies of all stationary points generated with the BP86/HF calculations were then recalculated with the BP86 functional, employing LANL2DZ pseudopotentials and basis sets for Rh and P (the latter with polarization) and 6-31G** basis sets on C, F, and H. These single point full DF energies are reported in the text. Calculations to assess the effects of solvation were performed using the polarized continuum model (PCM) approach[25] (benzene, ϵ = 2.24), and these showed the relative energies of the key transition states to be changed by less than 0.5 kcal/mol.

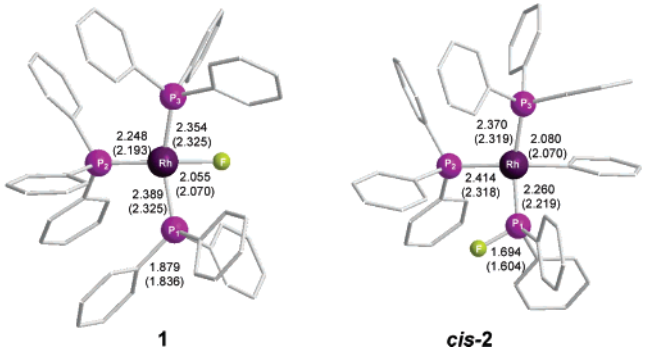

Figure 1. Computed geometries (Å) for [RhF(PPh$_3$)$_3$] (**1**) and *cis*-Rh(PPh$_3$)$_2$(PPh$_2$F)Ph (*cis*-**2**). Equivalent experimental values[12,13] are given in parentheses.

(17) Indeed, a barrier of only 1.8 kcal/mol for Ph group transfer in [PdH$_3$(PH$_2$Ph)]$^-$ model was reported. However, this figure is relative to a [PdH$_3$(PH$_2$Ph)]$^-$ reactant in which the PH-$_2$Ph ligand has a highly distorted geometry and so omits the energy associated with this reorganization.

(18) (a) Macgregor, S. A.; Neave, G. W. *Organometallics* **2004**, *23*, 891. (b) Braga, A. A. C.; Morgon, N. H.; Ujaque, G.; Maseras, F. *J. Am. Chem. Soc.* **2005**, *127*, 9298. (c) Kajiyama, K.; Nakamoto, A.; Miyazawa, S.; Miyamoto, T. K. *Chem. Lett.* **2003**, *32*, 332. (d) Mason, M. R.; Verkade, J. G. *Organometallics* **1992**, *11*, 2212.

(19) Frisch, M. J.; et al. *Gaussian 03*, revision C.02; Gaussian, Inc.: Wallingford, CT, 2004.

(20) Andrae, D.; Häusserman, U.; Dolg, M.; Stoll, H.; Preuss, H. *Theor. Chim. Acta* **1990**, *77*, 123.

(21) Höllwarth, A.; Böhme, M.; Dapprich, S.; Ehlers, A. W.; Gobbi, A.; Jonas, V.; Köhler, K. F.; Stegmann, R.; Veldkamp, A.; Frenking, G. *Chem. Phys. Lett.* **1993**, *208*, 237.

(22) (a) Hehre, W. J.; Ditchfield, R.; Pople, J. A. *J. Chem. Phys.* **1972**, *56*, 2257. (b) Hariharan, P. C.; Pople, J. A. *Theor. Chim. Acta* **1973**, *28*, 213.

(23) Hay, P. J.; Wadt, W. R. *J. Chem. Phys.* **1985**, *82*, 299.

(24) Pappu, R. V.; Hart, R. K.; Ponder, J. W. *J. Phys. Chem. B* **1998**, *102*, 9725.

(25) Cancès, M. T.; Mennucci, B.; Tomasi, J. *J. Chem. Phys.* **1997**, *107*, 3032.

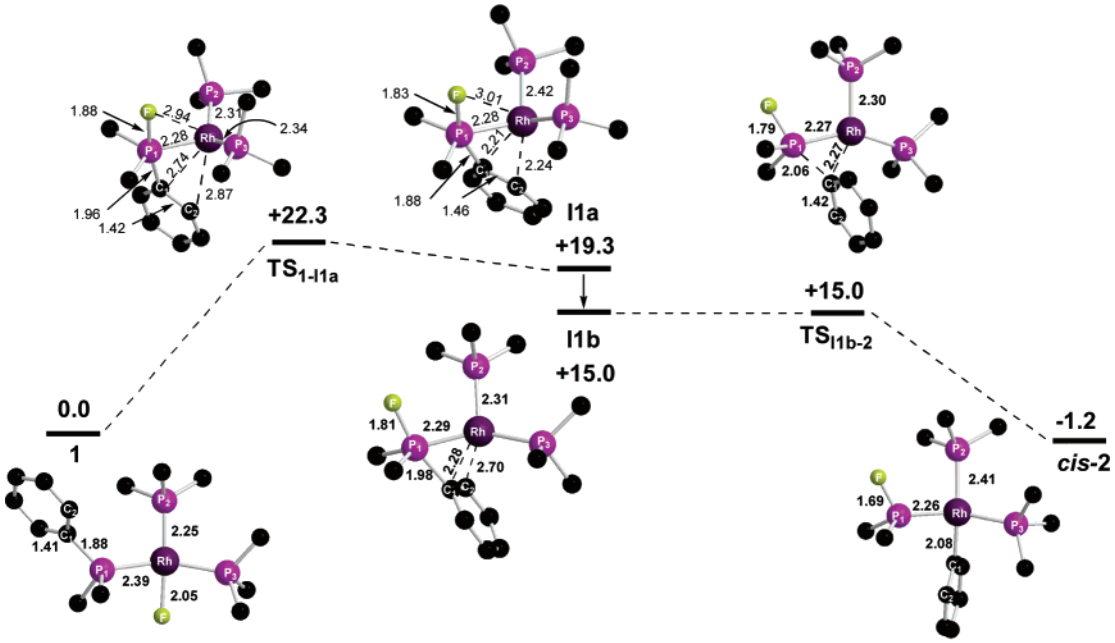

Figure 2. Computed reaction profile (kcal/mol) for F/Ph exchange in [RhF(PPh_3)$_3$] (**1**) via pathway 1a with key distances given in Å. Spectator phenyl substituents are truncated at the ipso carbon, and hydrogen atoms are omitted for clarity.

Results

To test the performance of the hybrid DFT/HF approach, the computed geometries of **1** and *cis*-**2** were compared with those determined crystallographically (see Figure 1).[12,13] The Rh−F (**1**) and Rh−Ph (*cis*-**2**) distances are well reproduced, as are the trends in Rh−P distances, with a shorter bond trans to fluoride in **1** and a longer Rh−P distance trans to Ph in *cis*-**2**, which also features a shorter Rh−PPh_2F bond. The Rh−P distances are, however, all somewhat overestimated by between 0.03 and 0.1 Å. This does not appear to reflect the BP86/HF methodology employed, as test calculations at the full DF theory level (BP86) did not show any significant change in the Rh−P distances. Moreover, a BP86/HF calculation on **1** where all Rh−ligand distances were fixed at their values determined experimentally gave a result only 1 kcal/mol higher in energy than the fully optimized structure. It appears therefore that the Rh−P bonds in **1** and *cis*-**2** (and related structures) are associated with a rather soft potential and that their elongation in the calculations will not contribute to a significant energetic error.

F/Ph Exchange via Metallophosphorane Species. Pathway 1a. The computed reaction profile for pathway 1a is presented in Figure 2, along with the associated atom numbering scheme. The initial transfer of fluoride onto a cis phosphine is accompanied by rotation about the Rh−P_1 bond to give a transition state (**TS$_{1-I1a}$**, E = +22.3 kcal/mol) featuring a 5-coordinate trigonal bipyramidal phosphorus center where fluoride and one phenyl group occupy the axial positions (F−P_1−Rh−P_2 = 84.1°). In addition, a rearrangement of the metal coordination geometry also occurs with the P_1−Rh−P_3 angle narrowing from 160° in **1** to 110° in **TS$_{1-I1a}$**. **TS$_{1-I1a}$** links to an intermediate, **I1a** (E = +19.3 kcal/mol), which retains an intact [$PFPh_3$] phosphoranide ligand but also features two short Rh−C distances (Rh−C_1 = 2.21 Å; Rh−C_2 = 2.24 Å). This indicates a degree of η^2-alkene interaction between Rh and the phenyl group, and this is supported by an elongation of the C_1−C_2 distance to 1.46 Å. Completion of F/Ph exchange requires transfer of the phenyl group to Rh; however, a transition state for this process could not be located directly from **I1a**. Instead an additional process corresponding to rotation about the Rh−P_1 bond was characterized, during which the phosphoranide ligand moves from a relatively upright orientation in **Int1a** (F−P_1−Rh−P_2 = 70.4°) through a transition state (E = +19.3 kcal/mol; F−P_1−Rh−P_2 = 59.0°; not shown in Figure 2) to a new intermediate **I1b** (E = +15.0 kcal/mol; F−P_1−Rh−P_2 = 27.9°). This process also results in the P_1−Rh−P_3 angle opening up to 146° creating a vacant site cis to the phosphoranide into which phenyl group transfer can take place. This final transfer occurs with virtually no barrier via **TS$_{I1b-2}$** (E = +15.0 kcal/mol) to give the F/Ph exchange product, *cis*-**2**.

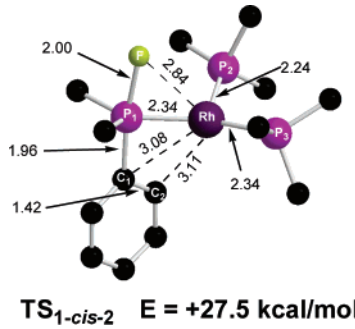

Figure 3. Computed structure of **TS$_{1-cis-2}$** for F/Ph Exchange in [RhF(PPh_3)$_3$] (**1**) via pathway 1b. Key distances given in Å. Spectator phenyl substituents are truncated at the ipso carbon, and hydrogen atoms are omitted for clarity.

Pathway 1b. This alternative pathway was found to involve a single transition state, **TS$_{1-cis-2}$** (E = +27.5 kcal/mol), which directly links **1** and *cis*-**2** (see Figure 3). **TS$_{1-cis-2}$** exhibits a metallophosphorane structure and is formed from **1** in a similar fashion to **TS$_{1-I1a}$** above, except that in this case no isomerization of the coordination geometry around Rh occurs (P_1−Rh−P_3 is only slightly reduced from 160° in **1** to 151° in **TS$_{1-cis-2}$**).

F/Ph Exchange via Rh(III)−Phosphido Species. Pathway 2a. Initial Ph group transfer from one of the *cis*-phosphine ligands in **1** to the Rh center entails an activation barrier of 33.3 kcal/mol (see Figure 4). In the transition state for this process, **TS$_{1-I2a}$**, the participating phosphine ligand has rotated to present one Ph group toward the metal, with the remaining

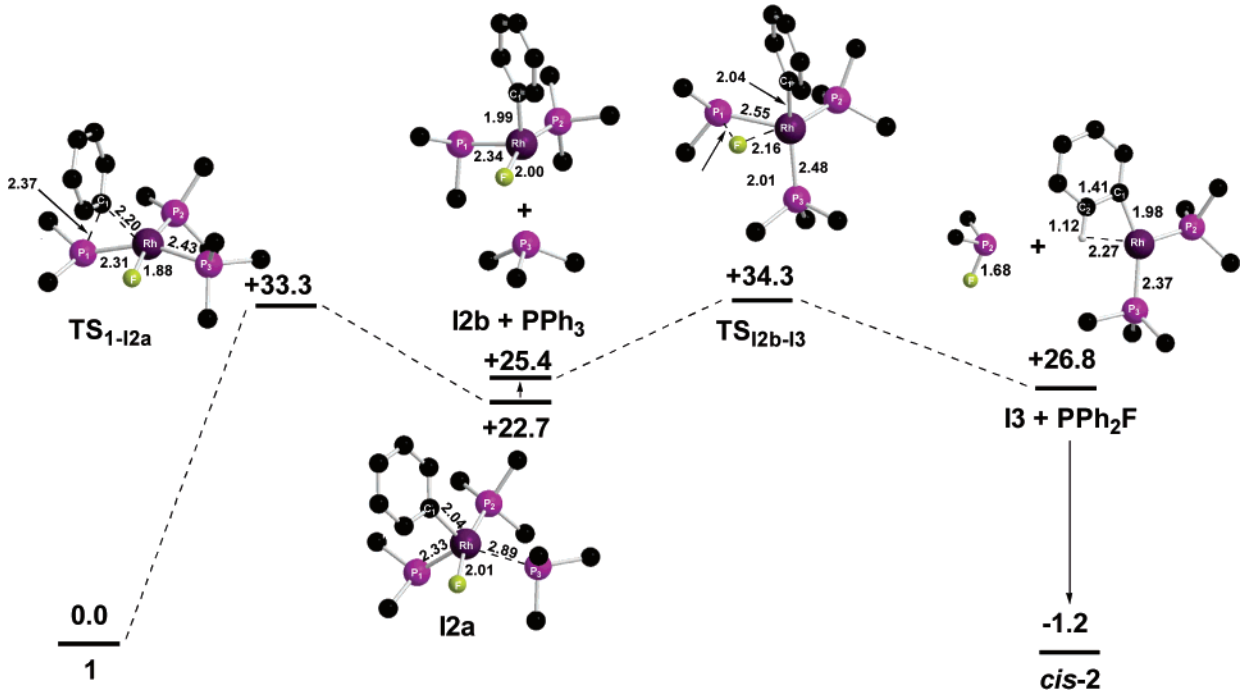

Figure 4. Computed reaction profile (kcal/mol) for F/Ph exchange in [RhF(PPh$_3$)$_3$] (**1**) via pathway 2a with key distances given in Å. Spectator phenyl substituents are truncated at the ipso carbon, and all hydrogen atoms are omitted for clarity.

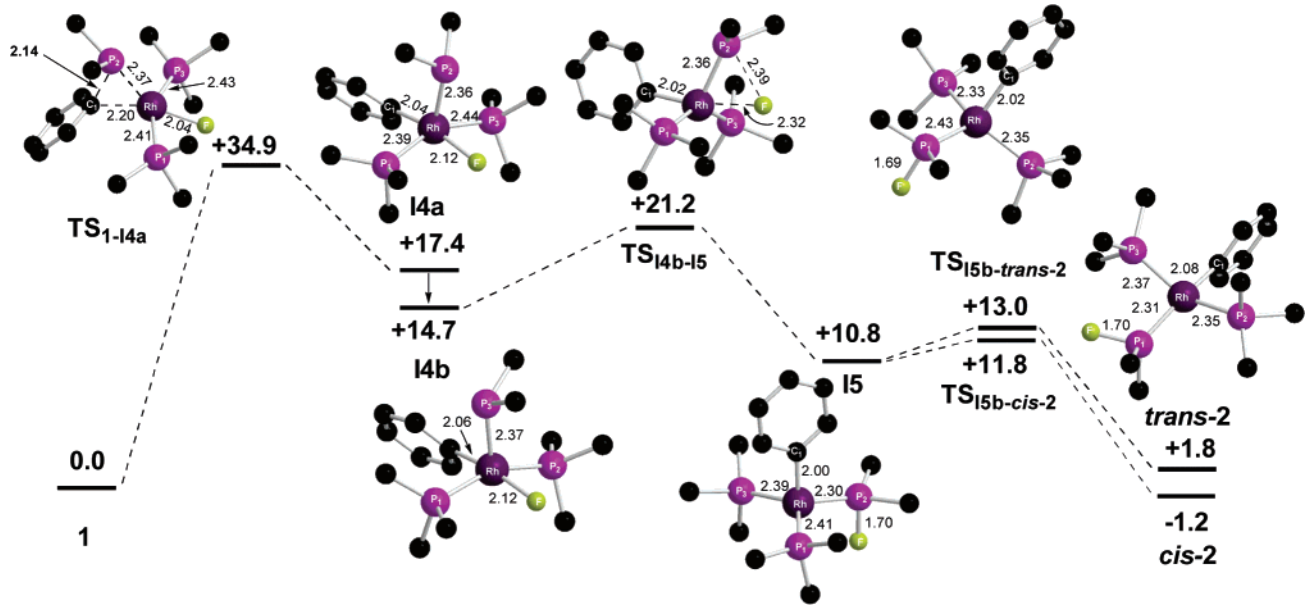

Figure 5. Computed reaction profile (kcal/mol) for F/Ph exchange in [RhF(PPh$_3$)$_3$] (**1**) via pathway 2b with key distances given in Å. Spectator phenyl substituents are truncated at the ipso carbon, and all hydrogen atoms are omitted for clarity.

PPh_2 moiety being staggered with respect to the forming Rh···C_1 bond. This arrangement is common to all the P−C activation (and the subsequent P−F bond forming) processes discussed here. During Ph group transfer a significant lengthening of the *trans*-Rh−P_3 bond is computed to 2.43 Å in **TS$_{1-I2a}$**, and this further increases to 2.89 Å in the initial intermediate formed (**I2a**, E = +22.7 kcal/mol). **I2a** is therefore best thought of as a 14e Rh(III) phosphido species with a loosely associated PPh_3 ligand. The d^6 [Rh(F)(Ph)(PPh_2)(PPh_3)] moiety in **I2a** adopts a butterfly structure with axial F and PPh_3 ligands and a tight equatorial P_1−Rh−C_1 angle of 96°. Similarly distorted geometries have been observed in the isoelectronic species [M(I^{t}Bu′)$_2$]$^+$ (M = Rh, Ir, where I^{t}Bu′ represents the cyclometallated 1,3-bis(*tert*-butyl)imidazol-2-ylidene ligand)[26] and [Ru(Ph)(CO)(P^{t}Bu$_2$Me)$_2$]$^+$.[27]

To complete Ph/F exchange from **I2a**, a P−F bond-forming step is required and a transition state for this formal reductive elimination was located (**TS$_{I2b-I3}$**, E = +34.3 kcal/mol). Characterization of **TS$_{I2b-I3}$**, however, indicated that it does not derive directly from **I2a** but from a new intermediate, **I2b** (E = +25.4 kcal/mol), in which the PPh_2 ligand is staggered with respect to the Rh−F bond and one PPh_3 ligand has now completely dissociated (Rh···P_3 > 4.5 Å). **I2b** is a rotamer of

(26) Scott, N. M.; Dorta, R.; Stevens, E. D.; Correa, A.; Cavallo, L.; Nolan, S. P. *J. Am. Chem. Soc.* **2005**, *127*, 3516.

(27) Huang, D.; Streib, W. E.; Eisenstein, O.; Caulton, K. G. *Angew. Chem., Int. Ed. Engl.* **1997**, *36*, 2004.

I2a, and the reorientation of the PPh_2 ligand appears sufficient to cause complete phosphine dissociation, although this process linking **I2a** to **I2b** was not studied further. The presence of the dissociated PPh_3 ligand in the calculations was necessary, however, to locate $\mathbf{TS_{I2b-I3}}$, as reaction profiles in its absence simply rose to very high energies without passing through any energy maximum. The P−F bond-forming step is therefore a ligand-assisted process in which the Rh−P_3 distance shortens to 2.48 Å in $\mathbf{TS_{I2b-I3}}$. This species also features a significant lengthening of both the Rh−P_1 and Rh−F bonds such that P−F bond formation results in dissociation of the newly formed $PFPh_2$ ligand. The remaining species, 14e $[RhPh(PPh_3)_2]$, **I3** ($E = +26.8$ kcal/mol, including free $PFPh_2$), is stabilized by an agostic interaction with one *o*-C−H bond of the Ph ligand. Addition of $PFPh_2$ to **I3** will lead to the F/Ph exchange product, *cis*-**2**, although this ligand addition process was not studied in any more detail.

Pathway 2b. In this process, initial P−C bond cleavage occurs from the phosphine ligand trans to F in **1**. This process is characterized by a shortening of the Rh···C_1 distance and movement of the PPh_2 moiety into an axial position in the eventual 5-coordinate intermediate formed, **I4a** (see Figure 5).

I4a is a stable square-pyramidal species and contrasts to the intermediates **I2a/b** located along pathway 2a where PPh_3 dissociation was seen. As in pathway 2a, rotation about the Rh−PPh_2 bond is required to orient the phosphido ligand in **I4a** for P−F bond formation. From this new rotamer (**I4b**, $E = +14.7$ kcal/mol) P−F bond formation occurs via $\mathbf{TS_{I4b-I5}}$ with an activation barrier of 6.5 kcal/mol, only slightly lower than the 8.9 kcal/mol computed for the equivalent step along pathway 2a. Consideration of the geometry of $\mathbf{TS_{I4b-I5}}$ might suggest that the product of P−F bond formation would be the trans isomer of **2**; however, instead an unexpected intermediate, **I5** ($E = +10.8$ kcal/mol), was located. **I5** exhibits an unusual trigonal geometry, related to a trigonal bipyramidal with Ph in one axial site but with the other axial position being vacant. Pathways linking **I5** to both *cis*- and *trans*-**2** were subsequently located with minimal activation barriers in both cases. This is illustrated in Figure 5 for the formation of *trans*-**2**; full details of $\mathbf{TS_{I5-}}_{\mathit{cis}\textbf{-2}}$ are given in the Supporting Information.

It is interesting to note that **I5** is actually an intermediate in the cis−trans isomerization of **2**. This process has been fully characterized by the present calculations and is closely related to the textbook square-planar−tetrahedral−square-planar mechanism.[28] Indeed, another view of **I5** could be as a flattened tetrahedron (the C_1−Rh−P angles average 98°), and its location as a local minimum may reflect the strong trans influence of the Ph ligand. The cis−trans isomerization of **2** via **I5** occurs with a rather low computed activation barrier of only 14.2 kcal/mol relative to the more stable cis isomer.

Discussion

The computed total activation energies for the four F/Ph exchange pathways are summarized in Table 1, where comparison is also made with the equivalent data from our previous study of the smaller model $[RhF(PH_3)_2(PH_2Ph)]$, **1′**.[13] The results for the full model system clearly indicate the most accessible mechanism is via pathway 1a. Moreover, the computed activation energy along pathway 1a is in excellent agreement with the experimental activation enthalpy of 22.0 ± 1.2 kcal/mol. Use of the full PPh_3 ligands is vital in obtaining this agreement, as it causes a significant reduction in activation energy for both metallophosphorane pathways, by about 10 kcal/mol. This is the key factor that differentiates pathway 1a from pathways 2a and 2b, as the decrease in activation energy along pathway 1a is reinforced by smaller increases along pathways 2a and 2b when the full model is employed.

Table 1. Computed Activation Energies (kcal/mol) for F/Ph Exchange via Pathways 1a and 1b and Pathways 2a and 2b in 1 and *cis*-1′[13,a]

	computed tot. activation energies (kcal/ mol)	
pathway	$[RhF(PPh_3)_3]$ (**1**)	$[RhF(PH_3)_2(PH_2Ph)]$ (**1′**)
1a (F to P transfer)	22.3	31.8
1b (F to P transfer)	27.5	37.3
2a (P−F formation)	34.3	32.3
2b (P−C activation)	34.9	31.7

[a] For each pathway the nature of the highest energy transition state is indicated in parentheses.

The key transition state along pathway 1a, $\mathbf{TS_{1-I1a}}$, features a metallophosphorane structure, and its formation involves a reorganization of the metal coordination geometry such that the $[PFPh_3]$ phosphoranide moiety is placed trans to the vacant site. This is consistent with $[PFPh_3]$ having a larger trans influence than PPh_3, and indeed, the alternative metallophosphorane transition state along pathway 1b, $\mathbf{TS_{1-}}_{\mathit{cis}\textbf{-2}}$, where PPh_3 is trans to the vacant site, is 5 kcal/mol less stable. Along pathway 1a two metallophosphorane intermediates, **I1a** and **I1b**, were located. However, the negligible barriers involved in their subsequent conversion to *cis*-**2** means that such species are unlikely ever to be isolatable. Stable metallophosphoranes generally feature electronegative substituents at phosphorus.[15] Examples of metallophosphoranes bearing aryl substituents have, however, been reported by Riess[6a] and Miyamoto,[18c] and in both cases, the transfer of an aryl group from phosphorus to metal appears to be facile, especially once a vacant site is created at the metal center. It is therefore not surprising that Ph transfer occurs so readily in **I1b** as it features a cis vacant site at Rh. This in turn suggests that blocking any available coordination sites may provide a means to stabilize metallophosphorane intermediates. In the absence of such stabilization, pathway 1a is probably best described as a concerted process in which F attack at P induces Ph transfer to Rh (cf. structure **A** in Scheme 2). This description certainly applies to pathway 1b where no metallophosphorane intermediates were located.

The reasons for the reduction in activation energies associated with the metallophosphorane pathways for **1** as compared to **1′** are not clear. Our computational approach means that both the electronic and steric effects of the Ph substituents in **1** are taken into account. On the basis of Tolman's electronic parameter, PPh_3 is expected to be somewhat more electron-rich than PH_3.[29] Therefore, intramolecular nucleophilic attack of F on PPh_3 in **1** might be expected to be less easy than on PH_2Ph in **1′**. In fact the calculations indicate the reverse to be true. One possible important difference in the structures of **1** and **1′** is a slight lengthening of the Rh−F bond, from 2.01 to 2.05 Å: the weakening of the Rh−F interaction that this implies may facilitate the key F to P transfer steps along pathways 1a and 1b. Alternatively, it may simply be that the inclusion of the full steric bulk of the PPh_3 ligands favors the reduction in metal coordination number that occurs when 3-coordinate structures such as the metallophosphorane-like $\mathbf{TS_{1-I1a}}$ and $\mathbf{TS_{1-}}_{\mathit{cis}\textbf{-2}}$ are formed.

(28) Atwood, J. D. *Inorganic and Organometallic Reaction Mechanisms*; Wiley-VCH: New York, 1997.

(29) Tolman, C. A. *Chem. Rev.* **1977**, *77*, 313.

Table 2. Computed Activation Barriers (kcal/mol) for P−C Activation and P−F Formation along Pathways 2a and 2b for 1 and *cis*-[RhF(PH$_3$)$_2$(PH$_2$Ph)], 1′[13]

	computed activation energies (kcal/mol)	
pathway	[RhF(PPh$_3$)$_3$] (**1**)	[RhF(PH$_3$)$_2$(PH$_2$Ph)] (**1′**)
2a (P−C activation)	33.3	24.7
2a (P−F formation)	8.9	19.9
2b (P−C activation)	34.9	30.0
2b (P−F formation)	6.5	12.3

Pathways 2a and 2b are based on initial P−C activation via Ph group transfer to give Rh−phosphido intermediates and for the full model system both are considerably less accessible than either metallophosphorane pathway. Pathways 2a and 2b each have similar total activation barriers of around 34 kcal/mol, although the nature of the high point along each differs (P−F formation along pathway 2a and P−C activation along pathway 2b). In addition to its high activation energy, pathway 2a also features two phosphine dissociation steps which suggest it cannot be operative for F/Ph exchange in **1**. The loss of PPh$_3$ after P−C activation would be inconsistent with the experimental kinetics of F/Ph exchange which showed no dependence on PPh$_3$ concentration. Moreover, the dissociation of PFPh$_2$ after P−F bond formation might be expected at higher PPh$_3$ concentration to result in the direct formation of some [RhPh(PPh$_3$)$_3$] and free PFPh$_2$, as the two phosphines compete for binding to the metal center in intermediate **I3**.

To investigate the factors controlling the total activation energies along pathways 2a and 2b it is instructive to consider the individual P−C activation and P−F forming steps involved. The relevant data for both **1** and **1′** are collected in Table 2, and this also gives us the opportunity to assess the energetics of these two fundamental processes. For **1′** P−C activation is more accessible when the PH$_2$Ph ligand is cis (E_a = 24.7 kcal/mol) rather than trans to fluoride (E_a = 30.0 kcal/mol). In the full model system both activation energies increase; however, this effect is greater for pathway 2a with the net result that very similar activation energies are computed for the *cis*- or *trans*-P−C activation steps. The electronic effect of introducing all the Ph groups in going from **1′** to **1** would be expected to be similar for both these processes. Therefore, the destabilization of the P−C activation transition states computed with **1** is apparently a steric effect, reflecting the fact that this process entails the system moving from 4- toward 5-coordinate. The greater destabilization for P−C activation along pathway 2a is probably due to the "fac" arrangement of bulky PPh$_3$ and PPh$_2$ ligands in **TS$_{1-12a}$**, as compared to their "mer" arrangement in **TS$_{1-14a}$** along pathway 2b. Thus, differential electronic and steric effects combine to make P−C bond activation equally accessible from either a cis or trans site in [RhF(PPh$_3$)$_3$].

The greater steric encumbrance along pathway 2a is also evident in the PPh$_3$ dissociation that occurs in **I2a**, and this can be compared with the intact square-pyramidal geometry that is maintained for **I4a** along pathway 2b. **I2a** (E = +22.7 kcal/mol) and **I4a** (E = +17.4 kcal/mol) are also both relatively destabilized than their analgoues computed with model **1′** (E = +10.4 and 13.1 kcal/mol, respectively;[13] once again this effect is greater along pathway 2a). The higher relative energies of these [RhF(Ph)(PPh$_2$)(PPh$_3$)$_2$] intermediates means that the subsequent P−F formation steps have lower activation energies when computed with the full model, **1**, than with **1′**. As this formal reductive elimination process results in a reduced coordination number, it will be favored by steric bulk, and the reduction in activation energy for this step is again more apparent along pathway 2a than pathway 2b.

Conclusions

In this study we have used DF calculations to show that F/Ph exchange in [RhF(PPh$_3$)$_3$] occurs via a novel metallophosphorane pathway. The inclusion of the full steric bulk of the phenyl substituents plays a crucial role in differentiating this pathway from alternatives based on initial P−C activation via Ph group transfer. This steric effect is linked to the reduction in metal coordination number that occurs during the formation of a metallophosphorane geometry, whereas Ph group transfer necessitates an increase in coordination number. The computed activation energy for F/Ph exchange is 22.3 kcal/mol, in excellent agreement with experimental value. The calculations indicate that the attack of a "hard" ligand such as fluoride at a neighboring phosphine can induce P−C bond activation with a much lower activation barrier compared to alternative pathways based on initial Ph group transfer to the metal. Such a process is potentially quite general and may play an important role in affecting the stability of metal−phosphine complexes in the presence of such "hard" donor species[3,6−10] and indeed may be related to aryl−aryl exchange reactions prevalent in Pd-mediated cross-coupling reactions.[4,5,11]

Acknowledgment. We thank Dr. Vladimir V. Grushin of Central Research and Development, E. I. Dupont de Nemours and Co., for many useful discussions. The funding of this work by the EPSRC via a postdoctoral fellowship (T.W.) is gratefully acknowledged. Computational resources on a HP/COMPAQ ES40 multiprocessor cluster (Columbus) at the Rutherford Appleton Laboratory (RAL), provided by the EPSRC National Service for Computational Chemistry Software, are acknowledged.

Supporting Information Available: Computed geometries of all species and related energies and a full ref 19. This material is available free of charge via the Internet at http://pubs.acs.org.

OM0610703